

TOWARDS SUSTAINABLE CENSUS INDEPENDENT POPULATION ESTIMATION IN MOZAMBIQUE

Isaac Neal¹, Sohan Seth^{1*}, Gary Watmough¹, Mamadou Saliou Diallo²

University of Edinburgh¹ and UNICEF²

{ineal, sseth, gary.watmough}@ed.ac.uk, mamsdiallo@unicef.org

ABSTRACT

Reliable and frequent population estimation is key for making policies around vaccination and planning infrastructure delivery. Since censuses lack the spatio-temporal resolution required for these tasks, census-independent approaches, using remote sensing and microcensus data, have become popular. We estimate intercensal population count in two pilot districts in Mozambique. To encourage sustainability, we assess the feasibility of using publicly available datasets to estimate population. We also explore transfer learning with existing annotated datasets for predicting building footprints, and training with additional ‘dot’ annotations from regions of interest to enhance these estimations. We observe that population predictions improve when using footprint area estimated with this approach versus only publicly available features.

1 INTRODUCTION

Accurate fine scale population estimates serve as a fundamental tool for policymakers. Many decisions involving access to services, distribution of vaccines and disaster relief, tracking of migration, and more are informed based on the most up to date population estimates for a region. Where these estimates are of insufficient resolution — either spatially or temporally — optimal decision making becomes difficult. Thus, there is a need for accurate and sustainable fine scale estimates of population globally, particularly in response to the COVID-19 pandemic, which requires efficient distribution of vaccines to vulnerable people, see e.g., Wang et al. (2020).

Over time, census data loses its resolution, both temporal and spatial, making it difficult to inform decision making for many of the problems mentioned above. Censuses are conducted infrequently, typically decennially, and due to privacy constraints, census data is typically unavailable to the wider community at the smallest administrative levels (Wardrop et al., 2018). Furthermore, census data can be inaccurate or incomplete due to budget limitations, lack of training, and socio-political circumstances (Wardrop et al., 2018), and may quickly become outdated due to conflicts, rapid migration or urban development, and disasters (Engstrom et al., 2020).

Census-independent population estimation (or bottom-up estimation) uses updated demographic information in periodic household surveys, or *microcensuses*, and detailed visual information offered by remote sensing technology to predict intercensal population density in non-surveyed areas. This approach could improve both temporal and spatial resolution of census data, since remote sensing data is available on a regular basis with sufficient resolution to estimate population at a fine scale. A summary of recent works in this area is provided in Table 1.

In this paper, we present ongoing work on bottom-up population estimation in Mozambique with a focus on *sustainability*. The goal is to establish a pipeline that can be maintained and used by non-experts over a long period, that relies on existing tools and datasets as much as possible, and requires minimal human supervision, e.g., in terms of annotation. We assess the feasibility of this approach, and find that building footprint area is a crucial attribute for estimating population. Moreover, building footprint area estimates using existing deep architecture and transfer learning are improved if additional annotated data is used from the region of interest (ROI). For greater sustainability, we suggest using easier ‘dot’ annotation (Lempitsky & Zisserman, 2010) for buildings from the ROI rather than more time-consuming polygon annotation which requires more human supervision.

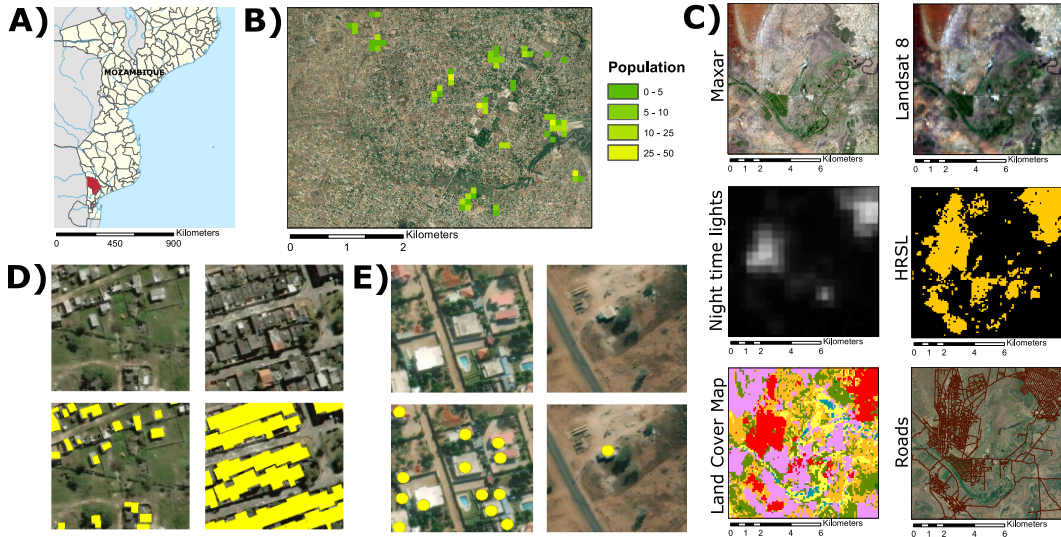


Figure 1: **A)** Regions of Mozambique (red) where microcensus was conducted, **B)** Distribution of gridded microcensus data in Boanne (BOA), **C)** Remote sensing data sources, **D)** Polygon building annotation from SpaceNet (100 m tiles), **E)** Dot building annotation from Mozambique (100 m tiles).

2 DATA AND PROCESSING

Microcensus: UNICEF funded a microcensus in 2019 conducted by SpaceSUR and GroundWork over two ROIs in Mozambique: Boanne (BOA) and Magude (MGD) (see Fig. 1A). The survey was conducted at a household level and households were exhaustively sampled over several primary sampling units (PSUs). We aggregated the household survey data to a 100 m grid to generate the response variable for predicting *gridded* population from remote sensing data (see Fig. 1B).

Remote Sensing: A variety of remote sensing imagery and derived data were used to model population count. The data sources are summarized in Table 2. Example images of each data source are shown in Fig. 1C. The 50 cm high-resolution satellite imagery (Vivid from Maxar) was a mosaic of WorldView-2 images, mostly from 2018 and 2019 (83% and 17% for BOA and 43% and 33% for MGD, remainder from 2011 to 2020). The night time lights (NTL) data was average intensity for the year 2019. The land cover classification was reclassified to condense forest types to *open forest* and *closed forest*. We ignored *no class*, *closed forest*, *herbaceous wasteland*, *moss*, *bare*, *snow*, *water*, and *sea* as they did not appear in our survey tiles. This left 5 classes. All raster data was reprojected to the 100 m survey grid for each ROI. Three types of resampling were used for different data-sources: average resampling for continuous data, nearest-neighbor resampling for coarser resolution categorical data, and any resampling (i.e. 1 if any underlying tile is 1 and otherwise 0) for finer resolution binary data.

Distance to Road Calculation: We rasterized the OSM road shapefiles to produce a Boolean raster indicating the presence of road in each grid tile, and calculated the Euclidean distance from each tile to the nearest tile with road as distance to road. We treated all road annotations from the OSM dataset the same, yielding one value for distance to road for each grid tile.

Building Footprint Identification We used a U-Net architecture (Ronneberger et al., 2015) with a VGG16 encoder (Simonyan & Zisserman, 2015) pre-trained on weights from ImageNet (Russakovsky et al., 2015) to segment an image into *building* and *non-building* areas. **BF1a)** We pre-trained the building footprint segmentation model on annotated satellite imagery from the SpaceNet challenge (Van Etten et al., 2019). We used the processed AOI 1 dataset from SpaceNet v1, which contains a large quantity of satellite imagery from Brazil with polygon building annotations. The dataset differs from our ROIs in Mozambique in several ways: SpaceNet tiles have more urban areas, a wetter climate, and different building colouration (see Figs. 1D-E). These factors hindered transfer learning between the tasks, and justified fine-tuning on a dataset from Mozambique. **BF1b)** We fine-tuned the model on ‘dot’ annotated buildings covering an area of 10 km² (i.e., 1,000 grid

Table 1: Summary of recent literature on topic of bottom up population estimation

	Weber et al. (2018)	Engstrom et al. (2020)	Hillson et al. (2019)	Leasure et al. (2020)
Region of Interest	Nigeria	Sri Lanka	Bo, Sierra Leone	Nigeria
Input Resolution	0.5 m (Maxar)	10 m (Polygon data) 12-30 m (Urban Footprint) 750 m (Night time Lights)	30 m (Landsat)	0.5m (Maxar), 100 m (WorldPop), various (OSM school density, household size)
Output Resolution	90 m	Village level	City district level	100 m
Input Data Cost	High (Maxar data)	Free (public data) High (Maxar data)	Free (public data)	Free (OSM, WorldPop) High (Maxar data)
Performance				
Validation	eTally data	Train/test split	LOOCV	Train/test split
MEAPE	-	28	11	-
R^2	0.98	0.58	-	0.26

NOTE: LOOCV = leave one out cross validation, MEAPE= median absolute percent error

Table 2: Remote sensing data sources, their characteristics and features extracted.

Data	Resolution	Year	Frequency	Prerequisite	Publicly avail. (source)	Features Extracted (Count)
Vivid Imagery	0.5 m	Various	4 d	N/A	No (Maxar)	Building area (1)
Landsat 8	30 m	2019	8 d	N/A	Yes (NASA/USGS)	10 bands, NDVI, NDWI (12)
High Resolution Settlement Layer	30 m	2015	N/A	High res. imagery and census data	Yes (CIESIN)	Binary Map (1)
Land cover classification	100 m	2019	Annual	Various	Yes (ESA)	LCC (5)
Night-time lights	750 m	2019	1 d	N/A	Yes (NOAA)	Radiance (1)
Road Data	Vector	Various	N/A	Volunteer annotation	Yes (OSM)	Distance to road (1)

NOTE: Although WorldView-2 imagery may be available every 4 days, we only had access to Vivid data from Maxar collected from various years. The number in parenthesis in the final column shows the number of derived features from that dataset.

tiles to reduce manual annotation) from the ROIs (outside surveyed areas to avoid data leakage). These annotations are a subset of those produced through a mixture of automatic estimation and manual curation in previous work by SpaceSUR. The ‘dot’ annotation was converted to raster class labels by rasterizing a circle around each point with the average area of buildings in the respective ROI. Dot annotation was preferred over polygon annotations to avail sustainability since the former is less time-intensive than the latter. This approach might not infer the exact boundary of a building but is only an intermediate step to population estimation.

Context Variable We introduced the notion of *context* to our model by calculating the average of each extracted feature (except distance to road) in the tiles surrounding the tile of interest (two surrounding contexts, 8 tiles and 24 tiles), and using these values as additional features in the model. In doing so, we aimed to provide the model with an understanding of the features on coarser scales.

Non-representative Tiles Upon investigating the data, we concluded that, due to the retrospective nature of the data, several tiles at the boundary of the PSUs only covered a PSU partially, and several surveyed areas had developed either before or after our high resolution satellite imagery was captured. This meant that the tiles often contained non-surveyed buildings or missing buildings, and therefore, our gridded data contained both developed tiles (i.e., with a large number of buildings) labeled as low population, and undeveloped tiles labeled as high population. Although it is possible to either automatically detect these ‘outlier’ tiles during training or use a robust loss function that is insensitive to them, it is not possible to validate a model on non-representative data. Therefore, we manually excluded these grid tiles from the data by comparing the surveyed buildings (GPS locations available in the microcensus) with those appearing in the Vivid imagery.

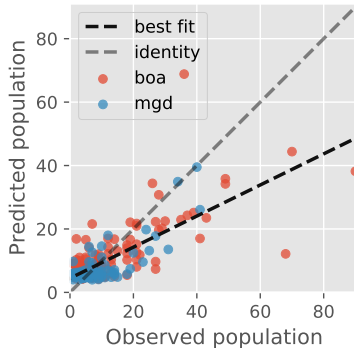
3 RESULTS AND DISCUSSION

Dataset We have 199 survey grid tiles and 61 predictor variables (see Table 2). **Cross-validation** Due to the limited quantity of data, we evaluated our population model through 4-fold cross validation. The data is split spatially into four approximately equal sized subsets (for each ROI separately), and we reported the error metrics over *pooled* prediction from the four validation folds. **Model** Due to the limited availability of data, we fit a single linear model with Huber loss function and ℓ_1 regularization (Yi & Huang, 2017) for both districts to model the log of population count given a combination of public features and BF1a or BF1b. We chose the model hyperparameters using 3-fold cross-validation over the training set for each fold of our spatial cross validation. **Evaluation Metrics** We chose several evaluation metrics, i.e., $R^2 = 1 - \frac{\sum_i (y_i - \hat{y}_i)^2}{\sum_i (y_i - \bar{y})^2}$, median absolute error MEAE = median $|y_i - \hat{y}_i|$, median absolute percentage error MEAPE = median $|y_i - \hat{y}_i|/y_i$, adjusted median absolute percentage error AMEAPE = median $|y_i - \hat{y}_i|/(y_i + 10)$ (to avoid division by zero), and aggregated percentage error AGGPE(A) = $|\sum_{i \in A} y_i - \sum_{i \in A} \hat{y}_i| / \sum_{i \in A} y_i$ (to capture error at a ROI level). **Null model** The null model predicted the population as the mean of the training set irrespective of the feature values. **Results** We observe that the model can effectively predict population, and outperforms the null model. The model performs the best with either public and fine-tuned building footprints (BF1b) as features, or only BF1b as features, and the performances are similar. A loss in accuracy is incurred when using either public only or public and pre-trained building footprints (BF1a) as features, however, the accuracy is still acceptable (MEAE is 3.8 versus 7.5 in null model). The model performed the worst when using only pre-trained building footprints (BF1a) as features, indicating that fine-tuning improves performance substantially.

Table 3: Summary of model performance

Features used	R^2	MEAPE	AMEAPE	MEAE	AGGPE
Public	0.05	51.8%	0.23	3.84	25.4%
BF1a	-0.08	59.9%	0.25	4.02	32.1%
BF1b	0.54	39.2%	0.20	3.41	14.9%
Public + BF1a	0.05	50.1%	0.23	3.97	27.3%
Public + BF1b	0.53	42.1%	0.19	3.45	13.2%
<u>Null Model</u>	-0.12	76.45%	0.41	7.57	1.68%

See **Evaluation Metrics** above for metric definitions. BF1a and BF1b are pre-trained and fine-tuned building area estimates respectively. Predicted vs. observed plot (**right**) summarizes the results for Public + BF1b.



We are currently addressing the following improvements to the model: **Buildings under construction** Our building segmentation model often identifies buildings that are under construction or buildings that are in ruin (e.g., historical buildings from colonial era with roof caved in). Since building footprint is an important feature in predicting population this can introduce bias in the outcome. We are improving the building segmentation model to help reduce this bias. **Non-residential buildings** Our building segmentation model does not discriminate between non-residential buildings (e.g., grain storage or schools) and residential buildings. We are addressing this by computing individual footprints prior to total area and discounting buildings that are too large or too small to likely be inhabited. **Distance to road** We treat all road types to be the same. We are extending this approach to give a more informative set of distance variables (e.g. distance to major highway) for different road types. We also intend to calculate road density to compare usefulness. **Sustainability** Sustainability is an issue in most bottom-up estimation techniques in the literature. The causes for this are twofold: the high cost of conducting population surveys, and limitations inherent to the machine learning methodology that might require expert annotation. Our results show that population can be estimated with limited survey data and ‘dot’ annotations. We are addressing this further by exploring ways to reduce dot annotation required. **External validation and transferability** It is difficult to externally validate the existing population estimation approaches or to compare them. This is because existing methods have been applied on different countries and a standard microcensus dataset does not exist for comparison. Furthermore, when microcensus data does exist it is difficult to access satellite images with the same spatial, temporal and radiometric characteristics using the Vivid data product. We are addressing this through conducting fresh microcensus surveys in Mozambique.

ACKNOWLEDGMENTS

The project was funded by the Data for Children Collaborative with UNICEF. The authors thank Pablo Martín Amieva (SpaceSUR) for his valuable insights on the project.

REFERENCES

- Ryan Engstrom, David Newhouse, and Vidhya Soundararajan. Estimating small-area population density in Sri Lanka using surveys and Geo-spatial data. *PLOS ONE*, 15(8):e0237063, August 2020. doi: 10.1371/journal.pone.0237063.
- Roger Hillson, Austin Coates, Joel D. Alejandro, Kathryn H. Jacobsen, Rashid Ansumana, Alfred S. Bockarie, Umaru Bangura, Joseph M. Lamin, and David A. Stenger. Estimating the size of urban populations using landsat images: a case study of bo, sierra leone, west africa. *International Journal of Health Geographics*, 18(1):16, July 2019. doi: 10.1186/s12942-019-0180-1.
- Douglas R. Leasure, Warren C. Jochem, Eric M. Weber, Vincent Seaman, and Andrew J. Tatem. National population mapping from sparse survey data: A hierarchical bayesian modeling framework to account for uncertainty. *Proceedings of the National Academy of Sciences*, 117(39):24173–24179, September 2020. doi: 10.1073/pnas.1913050117.
- Victor Lempitsky and Andrew Zisserman. Learning to count objects in images. In *Proceedings of the 23rd International Conference on Neural Information Processing Systems - Volume 1, NIPS'10*, pp. 1324–1332, 2010.
- Olaf Ronneberger, Philipp Fischer, and Thomas Brox. U-Net: Convolutional Networks for Biomedical Image Segmentation. In Nassir Navab, Joachim Hornegger, William M. Wells, and Alejandro F. Frangi (eds.), *Medical Image Computing and Computer-Assisted Intervention*, volume 9351, pp. 234–241. Springer International Publishing, Cham, May 2015. doi: 10.1007/978-3-319-24574-4_28. Series Title: Lecture Notes in Computer Science.
- Olga Russakovsky, Jia Deng, Hao Su, Jonathan Krause, Sanjeev Satheesh, Sean Ma, Zhiheng Huang, Andrej Karpathy, Aditya Khosla, Michael Bernstein, Alexander C. Berg, and Li Fei-Fei. ImageNet Large Scale Visual Recognition Challenge. *International Journal of Computer Vision (IJCV)*, 115(3):211–252, 2015. doi: 10.1007/s11263-015-0816-y.
- Karen Simonyan and Andrew Zisserman. Very deep convolutional networks for large-scale image recognition. In Yoshua Bengio and Yann LeCun (eds.), *3rd International Conference on Learning Representations, ICLR 2015, San Diego, CA, USA, Conference Track Proceedings*, May 2015.
- Adam Van Etten, Dave Lindenbaum, and Todd M. Bacastow. SpaceNet: A remote sensing dataset and challenge series. 2019.
- Wei Wang, Qianhui Wu, Juan Yang, Kaige Dong, Xinghui Chen, Xufang Bai, Xinhua Chen, Zhiyuan Chen, Cécile Viboud, Marco Ajelli, and Hongjie Yu. Global, regional, and national estimates of target population sizes for covid-19 vaccination: descriptive study. *BMJ*, pp. m4704, December 2020. doi: 10.1136/bmj.m4704.
- Nicola Wardrop, Warren Jochem, Tomas Bird, Heather Chamberlain, Donna Clarke, David Kerr, Linus Bengtsson, Sabrina Juran, Vincent Seaman, and Andrew Tatem. Spatially disaggregated population estimates in the absence of national population and housing census data. *Proceedings of the National Academy of Sciences*, 115(14):3529–3537, March 2018.
- Eric M Weber, Vincent Y Seaman, Robert N Stewart, Tomas J Bird, Andrew J Tatem, Jacob J McKee, Budhendra L Bhaduri, Jessica J Moehl, and Andrew E Reith. Census-independent population mapping in northern nigeria. *Remote sensing of environment*, 204:786–798, January 2018.
- Congrui Yi and Jian Huang. Semismooth Newton Coordinate Descent Algorithm for Elastic-Net Penalized Huber Loss Regression and Quantile Regression. *Journal of Computational and Graphical Statistics*, 26(3):547–557, July 2017. doi: 10.1080/10618600.2016.1256816.